ELSEVIER

Journal of Photochemistry and Photobiology A: Chemistry 146 (2001) 1–8

Journal of Photochemistry and Photobiology A:Chemistry

www.elsevier.com/locate/jphotochem

Laser induced fluorescence detection of CF, CF_2 and CF_3 in the infrared multiphoton dissociation of C_3F_6

L. Rubio*, M. Santos, J.A. Torresano

Instituto de Estructura de la Materia, Centro de Física Miguel A. Catalán, CSIC, Serrano 121, 28006 Madrid, Spain

Received 5 June 2001; accepted 27 August 2001

Abstract

The infrared multiphoton dissociation of C_3F_6 has been studied through the analysis of the laser induced fluorescence of the produced CF, CF_2 and CF_3 radicals. The influence of buffer gases in the process has also been investigated. In the studied conditions, only unimolecular formation of these radicals has been detected. A discussion about the possible dissociation channels has been done. The obtained excitation spectra show that CF_2 is formed vibrationally hot and reveal the presence of the radical CF_3. From the analysis of these spectra, different values of the vibrational temperature are obtained, for the two experimental employed arrangements.

Keywords: Laser induced fluorescence technique; Infrared multiphoton dissociation; Vibrational temperature

1. Introduction

The study of the infrared multiphoton dissociation (IRMPD) of perfluoropropene (C_3F_6) induced by one or two laser beams is interesting because this species can be used as a model molecule in the analysis of these processes. This is because the IRMPD behaviour of this molecule changes in a highly noticeable way by rather small variations in the irradiation conditions [1–3].

By using an extension of a quantitative method, previously developed by McRae et al. [4], we carried out, in previous works, the analysis of the contribution of the different collisional mechanisms to the IRMPD of C_3F_6 induced by one and two infrared laser beams, both for the neat molecule [2,3] and in the presence of Ar as a buffer gas [5,6]. It was shown that the loss of coherence in the absorption of the infrared radiation in this molecule strongly depends on the experimental parameters used in the irradiation, such as the laser fluence in one-beam irradiation experiments or the frequency of the second laser pulse in double-beam conditions. It was also found that the addition of Ar also affects the vibrational bottleneck, inducing the transition between the two regimes in which the IRMPD of C_3F_6 can operate [5,6].

To get a further insight into these processes, we have initiated a real time study of the IRMPD of C_3F_6 by the use of the laser induced fluorescence (LIF) technique. LIF allows to monitor in real time the production of radicals, providing valuable data about both the kinetics of the dissociation reactions and the nascent energy distribution among the produced fragments [7]. CF_2, the majority radical species produced in the IRMPD of C_3F_6, is readily detected by LIF. The CF_2 band system is well known and some of its electronic transitions posses a high quantum yield [8,9]. Indeed, the energy distribution of the IRMPD produced CF_2 has been obtained for a number of halogenated molecules [10–12]. The CF_3 radical is extremely weak fluorophore, and its detection by LIF, up to our knowledge, has not been reported. Usually, it has been observed in emission or by photofragment translational spectroscopy [13–17,47,48]. The CF radical has been the object of many experimental and theoretical studies, in particular the $A^2\Sigma^+$–$X^2\Pi$ transition [18–21,49].

The IRMPD of C_3F_6 was initially studied by Nip et al. [22]. They identified the C_2F_4 product in agreement with the main dissociation channel established from thermal experiments [23–25]. They proposed the following reaction:

$$C_3F_6 + nh\nu \rightarrow C_2F_4 + CF_2 \quad (1)$$

In these experiments, some amount of C_2F_6 was also detected. This was explained by postulating the reaction chain:

$$CF_2 + CF_2 \rightarrow CF_3 + CF \quad (2)$$

$$CF_3 + CF_3 \rightarrow C_2F_6 \quad (3)$$

These processes are favoured by the increase in pressure and/or fluence. The work carried out by our group lead to the detection of a solid dissociation final product identify as

* Corresponding author. Tel.: +34-1-564-5557; fax: +34-1-561-6800.
E-mail address: imtr424@iem.cfmac.csic.es (L. Rubio).

1010-6030/01/$ – see front matter
PII: S1010-6030(01)00590-1

poly-tetrafluoroethylene $(CF_2)_n$, which under certain conditions could represent up to 30% of the dissociated C_3F_6 [1].

Recently, Longfellow et al. [26] have studied the IRMPD of C_3F_6 by photofragment translational spectroscopy. Besides the primary reaction already discussed (1), they have identified a second primary channel which produces CF_3 and C_2F_3 by means of a simple bond rupture (4).

$$C_3F_6 + nh\nu \rightarrow C_2F_3 + CF_3 \quad (4)$$

They have also detected the CF_2 loss secondary channel (2), while no evidence of primary CF formation was found. With these results, the authors confirm the unimolecular dissociation of C_3F_6 by the primary channel (1) and observe for the first time the CF_3 formation in the unimolecular decomposition of this molecule (4).

The primary formation of the radical CF from C_3F_6 has been seen in the VUV photolysis of the C_3F_6 at 50 nm [27]. The authors propose two dissociation channels:

$$C_3F_6 + h\nu \rightarrow C_2F_5 + CF \quad (5)$$

$$C_3F_6 + h\nu \rightarrow C_2F_4 + CF + F \quad (6)$$

To study the radical formation in the IRMPD of C_3F_6, we have used the LIF technique analysing the unimolecular formation of vibrationally hot CF_2 radicals through its excitation spectrum. We have used the same technique to identify the CF and CF_3 radicals from the IRMPD of C_3F_6, and we have discussed the unimolecularity of these process.

2. Experimental

Lumonics K-103 and K-101 TEA CO_2 lasers are employed for the IRMPD of the C_3F_6 samples. They are equipped with frontal Ge multimode optics (35 and 85% reflectivity, respectively) and rear diffraction gratings with 135 lines/mm blazed at 10.6 μm. They are provided with low jitter trigger devices (Lumonics 524) supplying jitters between the IR and UV pulses lower than 100 ns in the pump and probe experiments.

Irradiation is carried out using the 9P(26) line at 1041 cm^{-1} of K-103 or K-101 instruments, nearly coincident with the C–F stretching mode of C_3F_6 [28]. The wavelength is checked with a 16-A spectrum analyser (Optical Eng.). The laser operates with a mixture of CO_2, N_2 and He in the proportion 8:8:84, the pulse temporal profile being monitored with a photon drag detector (Rofin Sinar 7415). The pulse consists in a spike varying from 40 to 80 ns (FWHM) and a tail lasting from 3 to 4 μs depending on the different wavelengths and lasers. When a tail-free pulse was needed, N_2 was removed from the gas mixture.

In general, the photolysis experiments are performed under gasflow conditions in a Pyrex cell of 4.5 cm diameter and 15.5 cm length, fitted with a pair of NaCl windows orthogonal to another pair of quartz windows.

Two different geometries are used, focused and near-parallel. In the first case, a 10 cm focal length lens is placed in front of the cell for both beams. In the second, 200 and 150 cm focal length lenses are used for K-103 and K-101 lasers, respectively, originating near-parallel beams along the cell.

The output of a N_2-pumped dye laser (PRA LN107 0.04 nm bandwidth, 500 ps temporal width) is frequency doubled though a KDP or a BBO crystals to produce around 10 μJ of tunable radiation in the 265–275 and 215–225 nm regions, respectively. In the first case, the radiation is isolated from the fundamental mode by a cut-off filter, while in the second case, a Pellin-Broca prism (Spectrosil) was necessary. The UV beam was focused, counter-propagating to the CO_2 laser beams, by a 50 cm quartz lens at the focus or at the centre of the infrared beam.

Photofragment fluorescence is collected through a quartz window at right angle to the laser axis and focused onto a 1P28 RCA or 928 Hamamatsu photomultiplier tubes. Spectral selection of the total produced fluorescence is carry out by using adequate interference or cut-off filters or a monochromator (Bausch and Lomb, 2700 lines/mm with a slit of 0.5 mm).

For all used experimental conditions, we have verified that a linear dependence exists between the probe laser intensity and the induced LIF intensity. We have worked with the usual assumption that the induced LIF intensity is proportional to the concentration of the excited states associated to the emission, and hence, to the radical ground state population.

The CO_2 laser pulse, picked up with the photon drag detector, triggers a Tektronix TDS 540 digital oscilloscope that is used to collect the signals and send them to a personal computer where they are averaged and analysed.

The delay between the CO_2 and the probe lasers is controlled by a Berkeley Nucleonics digital delay generator BNC 7036A to be within ∼50 ns. When no other specification is given this delay is kept at 800 ns.

The CO_2 laser fluence is calculated as the ratio of the pulse energy, as measured with Lumonics 20D pyroelectric detectors, and the 1/*e* cross-sectional beam area, measured at the cell position with a pyroelectric array Delta Development Mark IV. Measured areas for the different lasers,

Table 1
Measured beam areas for the employed lasers, wavelengths and geometries

Geometries	K-103 (cm^2)	K-101 (cm^2)
Focused	$(7.1 \pm 0.7) \times 10^{-3}$ (9.603 μm), $(9.3 \pm 0.9) \times 10^{-3}$ (10.148 μm)	$(5.8 \pm 0.6) \times 10^{-3}$ (9.603 μm)
Near-parallel	0.251 ± 0.013 (9.603 μm), 0.223 ± 0.011 (10.148 μm)	0.282 ± 0.014 (9.603 μm)

wavelength and geometries are given in Table 1. Each experimental point was obtained by averaging over 20 measurements. Sample pressures in the cell were measured with (0–1 and 0–10 hPa) MKS Baratron gauges. The dissociation yield was determined by infrared spectrophotometry, monitoring the change in the absorbance of the 1036 cm^{-1} band by using FTIR spectrophotometers, models Perkin Elmer 1725X or 1605.

C_3F_6 sample (99.0%) was purchased from ABCR chemicals and used without further purification.

3. Results and discussion

For the CF_2 detection, we have selected the $A^1B_1(0, 0, 0) \leftarrow (0, 0, 0)X^1A_1$ transition at 268.65 nm. The temporal profile of the CF_2 LIF signal consists in an initial spike that reach its maximum around 40 ns after the CO_2 pulse, followed by a small tail lasting less than 500 ns. These facts together with the absence of a second maximum at the time of the tail of the CO_2 pulse, indicate that secondary reactions or collisional processes are not involved in the formation of the CF_2 species, which can be considered as an unimolecular process in agreement with other real time detection of the CF_2 radical from IRMPD of C_3F_6 [22,26].

For all the used experimental conditions, we have obtained that the CF_2 LIF intensity always increases on the initial concentration of pure C_3F_6. However, the dependence of the relative LIF intensity, defined as the ratio of the intensity of the LIF signal to the initial pressure of C_3F_6, has the same qualitative behaviour found for the dissociation yield obtained from IR spectrometry of the stable final products at high fluence conditions [1]. This is, the yield decays when increasing the initial concentration of C_3F_6, in the studied pressure range. Therefore, the relative CF_2 LIF intensity can be considered as an approach to the net yield of the process of dissociation.

We have been able to carry out least-squared line fitting of the LIF signals to single exponential functions after the subtraction of a small background and the truncation of the perturbation induced by the laser spike. As it is expected from a non-collisional production of the fragments, the pressure of C_3F_6 corresponding to a null signal is 0.

We have obtained a non-collisional lifetime for the CF_2 first electronic state ($\tilde{A}(0, 0, 0)$ level) of 62 ± 4 ns in good agreement with the values given in the literature [9,29]. A quenching rate constant of $(7.1 \pm 0.7) \times 10^{13}\ s^{-1}\ mol^{-1}\ cm^3$ is obtained for the deactivation of this state through collisions with C_3F_6 molecules and the dissociation products. This value is comparable to those given for the quenching rate of CF_2 ($A(0, 6, 0)$) induced by C_2F_4 and CF_2Cl_2 [30]. The above data for lifetime and quenching rate correspond to parallel geometry experiments with a time delay between the photolysis and probe laser beams of 800 ns. For focused geometry and at the same time delay between both lasers, the obtained value for the quenching rate is $(1.2 \pm 0.7) \times 10^{14}\ s^{-1}\ mol^{-1}\ cm^3$. In this geometry, a larger density of dissociation products, mainly C_2F_4, are produced in the probed zone. The comparison between the quenching rate values for both geometries suggests that the quenching rate of the CF_2 fluorescence by C_3F_6 is smaller than by C_2F_4.

As it is well known [31], the presence of buffer gases inhibits the dissociation yield in the IRMPD of large molecules. We studied the influence of Ar in the behaviour of the C_3F_6 in relation to the dissociation process [5,6]. Now, we have measured the intensity of the obtained LIF signal when increasing the amount of argon, nitrogen or helium added to the sample in parallel geometry, and in static cell. In all the cases, the results show an exponential decrease of the LIF signal as the buffer pressure increases. These buffer gases essentially act relaxing the vibrationally excited molecules (C_3F_6 and/or products). When the relaxed molecule is C_3F_6, collisions with Ar, He or N_2 depopulate the region of energy above the dissociation threshold, quenching the dissociation yield. We have observed that the larger the fluence of the IR pulse the lower the Ar inhibition on the dissociation process. This is in agreement with the results establishing that collisions with buffers are more effective as lower is the excitation of the molecule [32]. On the other hand, since we are inducing the $A(0, 0, 0) \leftarrow X(0, 0, 0)$ transition, collisions with buffer depopulate the vibrationally excited levels leading to an increase of the probed vibrational ground state population. As the buffers do not quench the electronic excited state of CF_2 [33], the intensity of the LIF signal associated to this radical, is driven by the balance of dissociation quenching and vibrational relaxation. Therefore, due to the low dissociation threshold [26] and to the small vibrational relaxation rate constant of this radical [34], the inhibition of the dissociation is the predominant process leading to a decreasing plot of the CF_2 LIF signal intensity on the buffer pressure. The rate constants for this decrease are nearly the same for Ar and He while this value is a 50% smaller for N_2. As the amount of the buffer gas is increased, the lifetime of the signals also increases. This effect can be explained taken into account the larger quenching rate of the dissociation products, mainly C_2F_4, respect to the quenching rate of C_3F_6 cited above.

We have obtained the LIF excitation spectrum of CF_2 upon dissociation of C_3F_6 in the presence of Ar for focused and near-parallel geometry in static cell. It has been shown [10], that the CF_2 from the IRMPD of some molecules are created with such an excess of rotational energy that transitions from several vibronic bands overlap, giving rise to a nearly featureless excitation spectrum. To get a rather rotationally cold population of CF_2 radicals, besides the addition of argon, we have probed the fragments 22 μs after their formation, a time for which the diffusive removal of the formed species is still slow.

Fig. 1 gives the excitation spectra between 264 and 276 nm obtained in focused geometry with a wavelength step of 0.2 nm. A pressure of 5 hPa of C_3F_6 with Ar (0.36%) was employed. Each band contains transitions from a variety

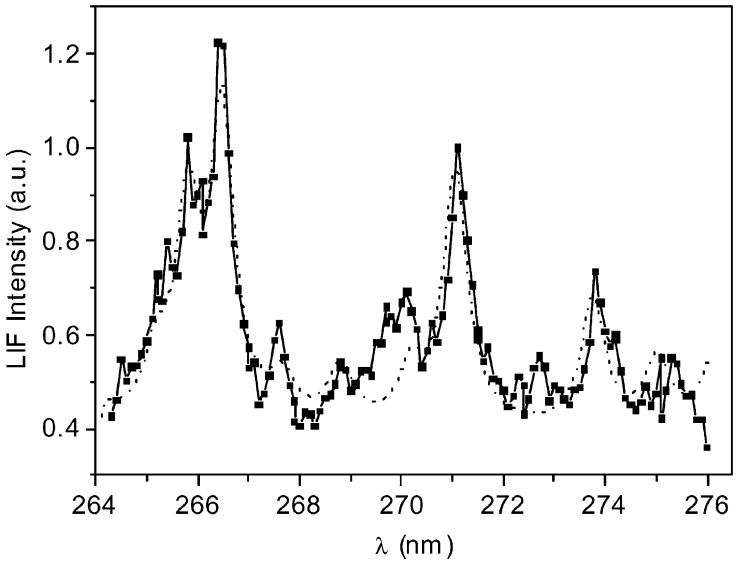

Fig. 1. LIF excitation spectrum of the CF_2 $\tilde{A}^1B_1$–X^1A_1 system from C_3F_6 dilute in Ar (0.36%) and in focused irradiation geometry. Dot line represents simulated spectrum.

of rotational states, unresolved with the best resolution of our dye laser, 0.04 nm. The experimental points have been normalised with the intensity of the dye laser, taking also into account the spectral response of the used filter.

We have compared the obtained spectrum with those given in the literature for LIF detection of CF_2 obtained from IRMPD experiments [8] and from reaction of metastable He and CF_2Cl_2 [9]. As it is expected, only the ν_2 mode is active [8,9]. Vibrational bands corresponding to the three sequences $\Delta\nu_2 = 0, 1, y - 1$ are obtained, clearly detecting the transitions for the levels 0, 1 and 2. Also transitions involving a higher vibrational quantum number have been detected in the same region. The assignations that we have done for the different CF_2 bands are given in Table 2 compared to those given in the literature. Vibrational temperature was measured by fitting a simulated spectrum to the experimental one (Fig. 1). Spectroscopic data used for simulation were taken from the literature [9,10,35]. The vibrational temperature, the bandwidth of the transitions and the measured experimental background were used as optimisation parameters. The fitting provides an estimation of 2500 K for the vibrational temperature in agreement with the value obtained for the same radical produced in the IRMPD of the CF_2CFCl [36]. As can be seen from the comparison of the experimental and simulated spectra, several features in our spectrum cannot be assigned to the CF_2 radical. There is a broad band in the region between 268.8 and 270.2 nm which does not correspond to any transition of the CF_2. Furthermore, the bands $A(0, 3, 0) \leftarrow X(0, 2, 0)$ and $A(0, 3, 0) \leftarrow X(0, 3, 0)$ of CF_2 at 267.6 and 272.7 nm, respectively, have in our spectrum a higher intensity that expected from the simulation. Later on we will discuss that these differences could be attributed to the presence of other species resulting from the IRMPD of C_3F_6, mainly the CF and CF_3 radicals.

As we have seen above, the LIF intensity of the CF_2 signal decreases when Ar is added. Therefore, the low fluence employed in near-parallel geometry, makes not possible to use the same C_3F_6 concentration for obtaining the excitation spectrum as it was done in focused geometry. As it is well known, Ar decreases the excited ro-vibrational population of the CF_2 produced in the IRMPD process [12,34]. So, a less amount of added Ar will produce a broadening of the vibrational structure of the spectrum. Fig. 2 shows the spectrum recorded in near-parallel geometry with 1% concentration of C_3F_6 in Ar and a time delay between IR and UV pulses of

Table 2
Assignations and intensities for the different bands of spectrum of Fig. 1

Bibliography	Assignation	Intensity	This work
	$\Delta\nu_2 = 0$		
275.5[a]	$(0, 6, 0) \rightarrow (0, 6, 0)$		275.3
275.24[b]	$(0, 5, 0) \rightarrow (0, 5, 0)$		275.3
273.76[b]	$(0, 4, 0) \rightarrow (0, 4, 0)$		273.8
272.68[b]	$(0, 3, 0) \rightarrow (0, 3, 0)$		272.7
271.06[b]	$(0, 2, 0) \rightarrow (0, 2, 0)$	++++	271.1
270.19[b]	$(0, 1, 0) \rightarrow (0, 1, 0)$	+++	270.1
268.74[a]	$(0, 0, 0) \rightarrow (0, 0, 0)$	+	268.8
	$\Delta\nu_2 = 1$		
270.19[a,b]	$(0, 4, 0) \rightarrow (0, 5, 0)$		270.1
268.9[b]	$(0, 3, 0) \rightarrow (0, 4, 0)$		268.8
267.68[b]	$(0, 2, 0) \rightarrow (0, 3, 0)$	++	267.6
266.48[b]	$(0, 1, 0) \rightarrow (0, 2, 0)$	+++++	266.4
265.39[b]	$(0, 0, 0) \rightarrow (0, 1, 0)$	++	265.8
	$\Delta\nu_2 = 1$		
273.76[b]	$(0, 1, 0) \rightarrow (0, 0, 0)$	+++	273.8
275.01[b]	$(0, 2, 0) \rightarrow (0, 1, 0)$	++	275.3

[a] Ref. [9].
[b] Ref. [10].

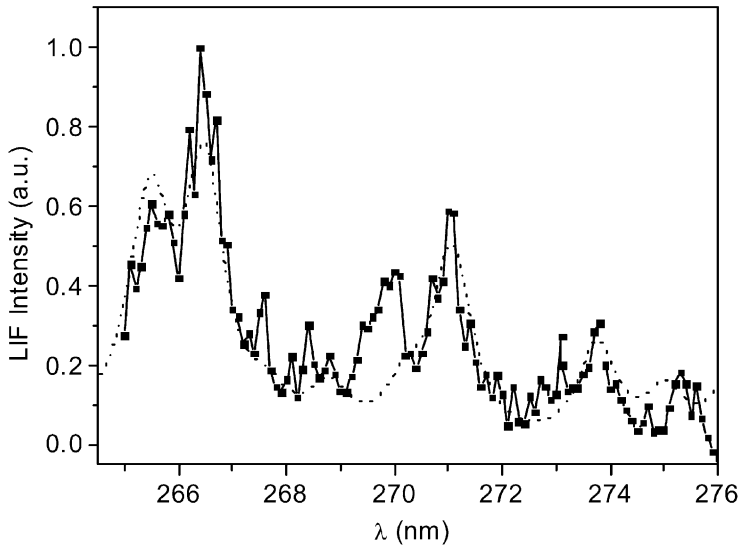

Fig. 2. LIF excitation spectrum of the CF_2 $\tilde{A}^1B_1$–X^1A_1 system from C_3F_6 dilute in Ar (1%) and in near-parallel irradiation geometry. Dot line represents simulated spectrum.

22 μs. The corresponding simulated spectrum is also shown. A larger bandwidth than in the focused case is obtained, suggesting a higher ro-vibrational excitation. The value obtained for the vibrational temperature in this case is 1900 K. As in the spectrum obtained in focused geometry, there are some features that cannot be assigned to the CF_2 radical.

Another radical produce in IRMPD of the C_3F_6 is fluorocarbene, CF, although it has not been directly detected [26]. Its spectroscopy has been widely studied [18–21,37,49]. We have selected the $A^2\Sigma^+(\nu' = 1) \leftarrow X^2\prod(\nu = 0)$ transition at 223.8 nm to investigate the presence of this radical because the CF_2 radical has very weak bands in this region [49]. At this wavelength we have obtained a signal similar to that of CF_2, but peaked around 12 ns. We have identify this signal first by measuring its non-collisional lifetime. The dependence of the lifetime of the LIF signal with the initial C_3F_6 pressure shows two regions separated by a threshold pressure of approximately 0.3 hPa. Below this value, the lifetime of the signal is nearly constant, indicating absence of collisions in this time. The radiative lifetime obtained is 26 ns in agreement with the lifetime for the CF radical given in the literature [18,20,38]. Above the 0.3 hPa region, the inverse of the lifetime linearly increase with pressure, providing a value for the quenching rate of CF by C_3F_6 and other present products of $8.75 \times 10^{14}\,\mathrm{mol^{-1}\,s^{-1}\,cm^3}$. A second identification of the signal is done from by the dispersion fluorescence spectrum obtained after exciting at the same wavelength (Fig. 3). In the figure it can be appreciated the

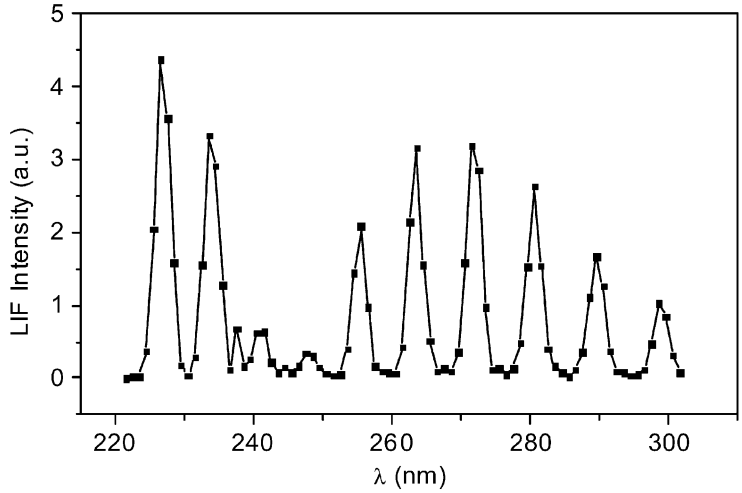

Fig. 3. LIF dispersion spectrum of CF radical obtaining by exciting the $A^2\Sigma^+(\nu' = 1) \leftarrow X^2\prod(\nu = 0)$ transition from pure C_3F_6 in focused irradiation geometry.

Table 3
Assignations and intensities for the different bands of spectrum of Fig. 2

Transition	This work (nm)	Bibliography (nm)
(1, 0)	225	225.4
(1, 1)	232	232.1
(1, 2)	239	239
(1, 3)	246	246.2
(1, 4)	254	253.8
(1, 5)	262	261.7
(1, 6)	270	270
(1, 7)	279	278.6
(1, 8)	288	287.7
(1, 9)	297	297.3

progression $\nu' = 1$, from $\nu'' = 0$ up to $\nu'' = 9$. In Table 3, the position of the bands, compared with the bibliography [39,49], are shown.

For all the used experimental conditions, we have found that the relative LIF intensity of the signal associated to the CF radical presents a similar behaviour to that obtained for the CF_2 radical. These measurements have been taken with a delay among the IR and probe pulses of 0.6 μs. In this interval of time, the evaluation of the collision frequency between C_3F_6 and all the other possible present species, shows that below an initial pressure of 0.1 hPa, no C_3F_6 collision has taken place. These facts, together with the similarity of both CF_2 and CF temporal profile signals, confirm the unimolecular formation of the CF radical. It is worth mentioning here that we have found identifiable CF LIF signal for IRMPD of C_3F_6 at pressures as low as 0.03 hPa.

The absorption electronic spectrum of the CF_3 radical has been studied by Glänzer and Maier [40] in the region 200–300 nm. These authors obtain the coefficient of absorption for CF_3 at 1300 K obtaining a structure with a broad maximum centred around 215 nm, although, the uncertainty in the measurements is high. The CF_3 radical is extremely weak fluorophore and its detection by LIF, up to our knowledge, has not been previously reported. Exciting at 218.8 nm, we observe a signal similar to those of CF_2 and CF, but peaked around 6 ns. In this region, the CF radical presents a band around 216 nm associated to the pre-dissociative level $\nu' = 2$ [49]. However, the weakness of this transition together with the lifetime of this level (2 ns), make possible to disregard any interference from the CF radical. The representation of the lifetime variation of the detected signal on the initial parent pressure shows a similar behaviour to that found for the CF radical. From the first constant region, a lifetime of 18 ns is obtained, which is very similar to the value given in the bibliography for the CF_3 radical (17.3 ns) [41].

The emission spectrum of CF_3 in the UV region 170–320 nm has been assigned to the transitions ($^2A_1' \rightarrow {}^1A_2''$), ($^2E \rightarrow {}^1A_2''$) and ($^2A_2 \rightarrow {}^1A_2''$) [13–15,47,48]. Of the four fundamental modes of the CF_3 radical, only transitions involving the ν_1 stretching and the ν_2 symmetric bending modes appear in the emission spectrum. According to Suto and coworkers, the value of 218.8 nm corresponds to the $(7, 0, 0, 0) \rightarrow (3, 0, 0, 0)$ transition. From these data we have assigned the observed signal to CF_3 formed vibrationally excited in the ground electronic state. We have calculated a value for the quenching rate of CF_3 by C_3F_6 and other present products of $7.11 \times 10^{14}\ mol^{-1}\ s^{-1}\ cm^3$.

Table 4
Dissociation energies for the different photolysis channels for C_3F_6. (1) and (4) are experimental [a Ref. 23, b Ref. 25, c Ref. 26]. The values associated to the CF formation are calculated from the heats of formation at 298 K, taken from [46]

Dissociation reaction	ΔH (kcal/mol)
$C_3F_6 + nh\nu \rightarrow C_2F_4 + CF_2$ (1)	75[a]; 82.7[b]
$C_3F_6 + nh\nu \rightarrow C_2F_3 + CF_3$ (4)	100–105[c]
$C_3F_6 + h\nu \rightarrow C_2F_5 + CF$ (5)	117
$C_3F_6 + nh\nu \rightarrow CF + CF_2 + CF_3$	171

The dependence of the relative LIF intensity associated to the CF_3 radical on the initial C_3F_6 pressure, as well as the temporal profiles of the signals, coincide with those obtained in the CF and CF_2 cases. The estimation of the collisions taking place in the formation-probe time interval provides the same conclusion found for the CF radical, i.e., collisions are not the responsible of the CF_3 formation.

To discuss the possible formation mechanisms for the radicals, we have summarised in Table 4, the dissociation channels proposed for the C_3F_6 together with their corresponding energy barriers. The formation of CF_2 and CF_3 radicals is explained by the established reactions (1) and (4). In the case of CF, the energy for its formation is higher than for CF_2 and CF_3. This is in agreement with the LIF intensity signal dependence on the irradiation fluence that we have obtained for the three radicals. We have found that an increase of the fluence favours the formation of CF in relation to the others, and also favours the formation of CF_3 in relation to CF_2. This behaviour suggests that reaction (2) is not the unique involved in the CF formation, but reactions (5) and (6) have also to be considered. Reaction (6) is unlikely in IR photolysis due to its high energy requirement.

Opposite to the LIF detection of CF_2, in the case of CF, an increase of the LIF intensity is obtained when the dissociation and excitation processes are carried out in the presence of Ar. The effect of an increase in the production of CF with fluence cited above, is in agreement with the high dissociation barrier expected for this radical (Table 4). This justify a weaker inhibitory action of Ar on the dissociation channel associated to CF formation. Furthermore, since we are inducing the $A^2\Sigma$–$X^2\prod(1 \leftarrow 0)$ transition, collisions with Ar depopulate the vibrationally excited levels leading to an increase of the vibrational ground state population. This effect prevails over the quenching of the dissociation, giving rise to the observed increase in the intensity. This fact suggests a higher relaxation rate constant for CF by Ar than for CF_2. To our knowledge, its value has not been measured.

The effect of Ar on the LIF signal intensity of the CF_3 radical is similar to that found in the case of CF_2. Since Ar does not quenches the emission of the electronically excited CF_3, the observed decrease indicates that the inhibitory effect onto the dissociation predominates over the vibrational relaxation, although this last mechanism is also present, as it will be discussed below.

The values obtained for the quenching rate for the CF and CF_3 radicals are quite similar and much larger than the one obtained for CF_2. It is not surprising due to the unreactive nature of this radical. Indeed, the recombination rate for CF_2 is two order of magnitude smaller than for CF_3 [42,43].

The CF_3 system presents several transitions overlapping the CF_2 bands in the region 264–275 nm [47]. These transitions involve highly excited vibrational levels. The transitions (12, 2, 0, 0)–(0, 0, 0, 0) and (14, 0, 0, 0)–(1, 0, 0, 0) at 269.55 and 268.95 nm, respectively, are in a region where do not exist any attributable transitions to the CF_2 radical. In this region appears the broad band found in our spectra between 268.8 and 270.2 nm. The existence of the (13, 1, 0, 0)–(0, 0, 0, 0) and (13, 0, 0, 0)–(0, 0, 0, 0) CF_3 transitions at 272.2 and 267.8 nm, respectively, could explain the discrepancies that we have observed in the relative intensity of the CF_2 transitions A(0, 3, 0)–X(0, 3, 0) and A(0, 2, 0)–X(0, 1, 0) at 272.48 and 267.68 nm, respectively. Furthermore, the differences between both experimental and simulated spectra at wavelengths below 268 nm (Fig. 2) could be due to the CF_3 transition (13, 1, 0, 0)–(1, 0, 0, 0) at 266.4 nm. This finding confirms the conclusion made above that the signal observed when exciting at 218.8 nm corresponds to the CF_3 radical. From the comparison of experimental spectra shown in Figs. 1 and 2, it is detected a more evident presence of CF_3 in the near-parallel case. This could be due to the less vibrational relaxation induced by Ar in CF_2 than in CF_3, as can be seen from the corresponding vibrational relaxation rates [34,44,45]. The presence of CF_3 broadens the spectrum profile and, as a consequence, the given values for the vibrational temperature could be larger than the real ones.

4. Conclusions

In this work, we have used the LIF technique to detect the CF, CF_2 and CF_3 radicals produced in the IRMPD of C_3F_6, being the first report of CF_3 detection by LIF. The CF radical has been identified by its non-collisional lifetime and trough its dispersion spectrum obtained by exciting the (1–0) band. The CF_3 radical has been uncovered also from its non-collisional lifetime and by its interference in the CF_2 spectra. The CF_3 presence is higher in the spectrum obtained at lower fluence and vibrational relaxation. We have confirmed that the CF_2 and CF_3 radicals are formed from primary and unimolecular channels. We have proposed the existence of a similar mechanism for the CF production.

From the analysis of the excitation spectra of the radical CF_2, we have concluded that it is formed vibrationally excited. We have obtained the vibrational temperature for this radical in our experimental conditions.

References

[1] J.A. Torresano, M. Santos, P.F. González-Díaz, Laser Chem. 14 (1994) 17.
[2] J.A. Torresano, M. Santos, J. Phys. Chem. 100 (1996) 9726.
[3] J.A. Torresano, M. Santos, J. Phys. Chem. A 101 (1997) 2221.
[4] G.A. McRae, P.E. Lee, R.D. McAlpine, J. Phys. Chem. 95 (1991) 9332.
[5] J.A. Torresano, M. Santos, Chem. Phys. Lett. 277 (1997) 39.
[6] L. Rubio, M. Santos, J.A. Torresano, Laser Chemistry, in press.
[7] D.W. Lupo, M. Quack, Chem. Rev. 87 (1987) 181.
[8] D.S. King, P.K. Schenck, J.C. Stephenson, J. Mol. Spectrosc. 78 (1979) 1.
[9] T. Ishiguro, Y. Hamada, M. Tsuboi, Bull. Chem. Soc. Jpn. 54 (1981) 367.
[10] J.C. Stephenson, D.S. King, J. Chem. Phys. 69 (1978) 1485.
[11] J.C. Stephenson, S.E. Bialkowski, D.S. King, J. Chem. Phys. 72 (1980) 161.
[12] W. Strube, J. Wollbrandt, M. Rossberg, E. Linke, J. Chem. Phys. 105 (1996) 9478.
[13] M. Suto, N. Washida, J. Chem. Phys. 78 (1983) 1007.
[14] N. Washida, M. Suto, S. Nagase, U. Nagashima, K. Morokuma, J. Chem. Phys. 78 (1983) 1025.
[15] C. Larrieu, M. Chaillet, A. Dargelos, J. Chem. Phys. 96 (1992) 3732.
[16] C.R. Quick Jr., J.J. Tiee, Chem. Phys. Lett. 114 (1985) 371.
[17] R.W. Dreyfus, L. Urbach, Chem. Phys. Lett. 114 (1985) 376.
[18] A.P. Rendell, C.W. Bauschlicher, S.R. Langhoff, Chem. Phys. Lett. 163 (1989) 354.
[19] M. Roßberg, W. Strube, J. Wollbrandt, E. Linke, J. Photochem. Photobiol. 80 (1994) 61.
[20] J.P. Booth, G. Hancock, Chem. Phys. Lett. 150 (1988) 457.
[21] I.D. Petsalakis, J. Chem. Phys. 110 (1999) 10730.
[22] W.S. Nip, P.A. Hackett, C. Willis, J. Phys. Chem. 84 (1980) 932.
[23] B. Atkinson, A.B. Trenwith, J. Chem. Soc. (1957) 2082.
[24] R.A. Matula, J. Phys. Chem. 72 (1968) 3054.
[25] N.N. Buratsev, A.S. Grigor'ev, Y.A. Kolbanovskii, Kinet. Catal. 30 (1989) 13.
[26] C.A. Longfellow, L.A. Smoliar, Y.T. Lee, Y.R. Lee, C.Y. Yeh, S.M. Lin, J. Phys. Chem. A 101 (1997) 338.
[27] G.K. Jarvis, K.J. Boyle, C.A. Mayhew, R.P. Tuckett, J. Phys. Chem. A 102 (1998) 3230.
[28] J.R. Nielsen, H.H. Claasen, H.H. Smith, D.C. Smith, J. Chem. Phys. 20 (1952) 1916.
[29] F.B. Wampler, J.J. Tiee, W.W. Rice, R.C. Oldenborg, J. Chem. Phys. 71 (1979) 3926.
[30] W. Hack, W. Langel, J. Photochem. 21 (1983) 105.
[31] C.D. Cantrell (Ed.), Multiple Photon Excitation and Dissociation of Polyatomic Molecules, Topics in Current Physics, Vol. 35, Springer, Berlin, 1986.
[32] M.A. Blitz, M. Pesa, M.J. Pilling, P.W. Seakins, Chem. Phys. Lett. 322 (2000) 280.
[33] G. Dornhöfer, W. Hack, W. Langel, J. Phys. Chem. 87 (1983) 3456.
[34] S.E. Bialkowski, D.S. King, J.C. Stephenson, J. Chem. Phys. 72 (1980) 1156.
[35] K.A. Peterson, R.C. Mayrhofer, E.L. Sibert III, R.C. Woods, J. Chem. Phys. 94 (1991) 414.
[36] J.C. Stephenson, D.S. King, J. Chem. Phys. 78 (1983) 1867.
[37] F.J. Grieman, A.T. Droege, P.C. Egelking, J. Chem. Phys. 78 (1983) 2248.
[38] D. L'Espérance, B.A. Williams, J.W. Fleming, Chem. Phys. Lett. 280 (1997) 113.

[39] T.L. Porter, D.E. Mann, N. Acquista, J. Mol. Spectrosc. 16 (1965) 228.
[40] K. Glänzer, M. Maier, J. Troe, J. Phys. Chem. 84 (1980) 1681.
[41] J.C. Creasey, I.R. Lambert, R.P. Tuckett, A. Hopkirk, Mol. Phys. 71 (1990) 1355.
[42] F. Battin-Leclerc, A.P. Smith, G.D. Hayman, T.P. Murrells, J. Chem. Soc., Faraday Trans. 92 (1996) 3305.
[43] J.J. Orlando, D.R. Smith, J. Phys. Chem. 92 (1988) 5147.
[44] M.A. Young, G.C. Pimentel, J. Phys. Chem. 94 (1990) 4884.
[45] M. Suh, W. Sung, S. Heo, H. Hwang, J. Phys. Chem. 103 (1999) 8365.
[46] S.G. Lias, J.E. Bartmess, J.F. Liebman, J.L. Holmes, R.D. Levin, W.G. Mallard, J. Phys. Chem. Ref. Data Vol. 17 (Suppl. 1) (1988).
[47] M. Suto, N. Washida, J. Chem. Phys. 78 (1983) 1012.
[48] M. Suto, N. Washida, H. Akimoto, M. Nakamura, J. Chem. Phys. 78 (1983) 1019.
[49] J.P. Booth, G. Hancock, M.J. Toogood, K.G. McKendrick, J. Phys. Chem. 100 (1996) 47.